Frequency-agile, rapid scanning spectroscopy: absorption sensitivity of 2×10^{-12} cm^{-1} Hz$^{-1/2}$ with a tunable diode laser

**D. A. Long · G.-W. Truong · R. D. van Zee ·
D. F. Plusquellic · J. T. Hodges**

Abstract We present ultrasensitive measurements of molecular absorption using frequency-agile rapid scanning, cavity ring-down spectroscopy with an external-cavity diode laser. A microwave source that drives an electro-optic phase modulator with a bandwidth of 20 GHz generates pairs of sidebands on the probe laser. The optical cavity provides for high sensitivity and filters the carrier and all but a single, selected sideband. Absorption spectra were acquired by stepping the tunable sideband from mode-to-mode of the ring-down cavity at a rate that was limited only by the cavity decay time. This approach allows for scanning rates of 8 kHz per cavity resonance, a minimum detectable absorption coefficient of 1.7×10^{-11} cm^{-1} after only 20 ms of averaging, and a noise-equivalent absorption coefficient of 1.7×10^{-12} cm^{-1} Hz$^{-1/2}$. By comparison with cavity-enhanced laser absorption spectrometers reported in the literature, the present system is, to the best of our knowledge, among the most sensitive and has by far the highest spectrum scanning rate.

1 Introduction

At present, there are many problems in trace gas sensing and chemical physics that require ultrasensitive spectrometers with a fast response and the ability to precisely measure absorption spectra. Cavity-enhanced laser absorption measurements exploit the long effective path lengths of high-finesse optical resonators to yield low detection limits and high spectral resolution [1–8]. However, in typical implementations, these instruments have relatively slow scanning rates. In the case of a continuously swept probe laser and a fixed-length resonator, this situation effectively reduces the measurement duty cycle and can lead to spectral distortion [9, 10]. Alternatively, when the resonator's length (and hence resonant frequency) is swept, mechanical elements limit both the rate and range of tuning [11]. In summary, for cavity-enhanced spectroscopic techniques, there are important tradeoffs with regard to optimizing sensitivity, duty cycle, spectral fidelity, and wavelength coverage.

We have recently presented a new approach to cavity-enhanced spectroscopy in which high-bandwidth electro-optics are utilized to *step* a selected laser sideband from mode-to-mode of a resonant cavity and thus scan across a molecular resonance [12]. This technique, which we refer to as frequency-agile, rapid scanning spectroscopy (FARS), removes the dead time associated with tuning the laser frequency between the resonances of a high-finesse cavity and thus yields scanning rates that are limited only by the cavity response time. While our initial demonstrations achieved high sensitivities and scanning rates, we utilized distributed feedback and ultranarrow linewidth fiber lasers that offer tuning ranges of only a few nanometers.

Herein, we describe a realization of FARS cavity ring-down spectroscopy (FARS-CRDS) that utilizes a commercially available and widely tunable external-cavity diode laser (ECDL). This experiment uses two orthogonal, linear polarizations of the probe laser: one providing a continuous high-bandwidth lock to the ring-down cavity,

D. A. Long (✉) · G.-W. Truong · R. D. van Zee ·
D. F. Plusquellic · J. T. Hodges
National Institute of Standards and Technology,
100 Bureau Drive, Gaithersburg, MD 20899, USA
e-mail: david.long@nist.gov

G.-W. Truong
Frequency Standards and Metrology Research Group,
School of Physics, The University of Western Australia,
Perth, WA 6009, Australia

and the other being stepped from mode-to-mode of the ring-down cavity and across a molecular absorption resonance. We quantify the sensitivity, scanning rate and spectral fidelity of the technique, and we compare these results to previous cavity-enhanced methods. The broad tuning range (≈ 60 nm) of ECDLs and their availability in the visible through near-infrared wavelength ranges is expected to enable FARS-CRDS measurements of numerous molecular species.

2 Experiment

These measurements were performed at the National Institute of Standards and Technology (NIST) in Gaithersburg, Maryland. We used a symmetric two-mirror optical cavity with a free spectral range f_{FSR} of ≈ 200 MHz and a finesse of $\approx 20,000$. Ring-down signals were measured with a commercial DC-coupled InGaAs photoreceiver (bandwidth = 8 MHz, measured noise-equivalent power = 18 pW Hz$^{-1/2}$, continuous wave saturation power at 1,600 nm = 10 mW) and digitized using a 16-bit board with a sampling rate of 25 Ms/s. For long-term measurements, we stabilized the cavity's length (and therefore its resonant frequencies) with respect to an I$_2$-stabilized HeNe laser (see Refs. [3, 13] for further details on this technique). We used a commercial, fiber-coupled ECDL with an output power of ≈ 25 mW, a free-running linewidth of ≤ 200 kHz, and a wavelength tuning range between 1,570 and 1,630 nm. The output was split into probe and locking legs (see Fig. 1) having orthogonal, linear polarizations [5, 14].

The lock beam was modulated with a waveguide electro-optic phase modulator (denoted EOM1) to produce fixed frequency sidebands at $f_{m,0} = \pm 13$ MHz relative to the carrier frequency in order to facilitate Pound–Drever–Hall (PDH) locking [15] of the laser to the optical cavity. Unlike conventional PDH locking, which stabilizes the laser carrier to a given cavity resonance, we locked one of the sidebands of the locking beam to the optical cavity. This ensures that the carrier frequency (for both the probe and locking legs) is nonresonant.

This offset lock was performed by demodulating the PDH photodiode signal (PD1) at a frequency of $2f_{m,0}$. The use of second-order demodulation is convenient as the error signal is proportional to the amplitudes of the two first-order sidebands and is independent of the carrier amplitude. In contrast to a traditional PDH lock, the two sideband error signals have opposite slopes as depicted in the lower panel of Fig. 1; therefore, by setting the feedback polarity, we can ensure that we always lock to a particular sideband.

The probe beam was also phase modulated with a waveguide electro-optic modulator (denoted EOM2) to produce tunable sidebands. The modulation frequency was supplied by a microwave source with a bandwidth of 20 GHz and a switching time of 100 μs. At each microwave frequency, the modulation amplitude was adjusted so that the carrier and first-order sidebands had similar amplitudes. The microwave frequency (f_{MW}) was then set to:

$$f_{MW} = nf_{FSR} \pm f_{m,0} \tag{1}$$

where n is the integer step number and the sign of the $f_{m,0}$ term is set based upon the desired lock sideband (and is held constant once the lock phase is set). As illustrated in Fig. 1, the cavity filters out all the frequency components (including higher-order sidebands) of the modulated laser except for the selected sideband for any choice of n (with an appropriately chosen $f_{m,0}$). Ring-down events were initiated by the use of a microwave switch (extinction of -80 dB) which turned off the microwave signal driving EOM2 within 20 ns. This approach eliminates the need for an acousto-optic modulator (AOM) to serve as a high-bandwidth optical switch [16].

In the first realization of the FARS technique [12], the probe and cavity frequencies were separately referenced to independent optical sources: the probe to an optical frequency comb (OFC) and the cavity to an I$_2$-stabilized HeNe laser. Herein, we have instead adopted a self-referenced approach in which the probe source is directly locked to the measurement cavity [14]. This simplified locking design removes the requirement for two tight locks to two high-quality (low noise and low drift) references.

The high-bandwidth PDH servo provides a tight lock of the probe laser frequency to the resonator. Importantly, since the probe and locking legs have orthogonal polarizations, it is not necessary to interrupt the PDH lock during a ring-down event. This type of dual-polarization, continuous PDH lock [14] is far simpler and more robust than other approaches that require constant interruption and reacquisition of the PDH lock (e.g., [4, 17]).

This configuration provides common mode rejection of amplitude noise in the transmitted laser power, caused by fluctuations in the frequencies of the laser and cavity resonances. In order to measure the power spectral density (PSD) of these fluctuations and to quantify the relative linewidth of the PDH-locked laser, we tuned EOM2 so that one sideband of the ECDL was positioned at the mid-point intensity of a cavity mode and therefore acted as a frequency discriminator when observed in transmission through the ring-down cavity. The measured PSD is shown in the upper panel of Fig. 2 and yields a relative linewidth for the PDH-locked laser of ≈ 130 Hz, which ensures efficient coupling of the probe laser into the ring-down cavity. As discussed below, the tightly locked laser also enables accurate determination of the free spectral range and total cavity losses.
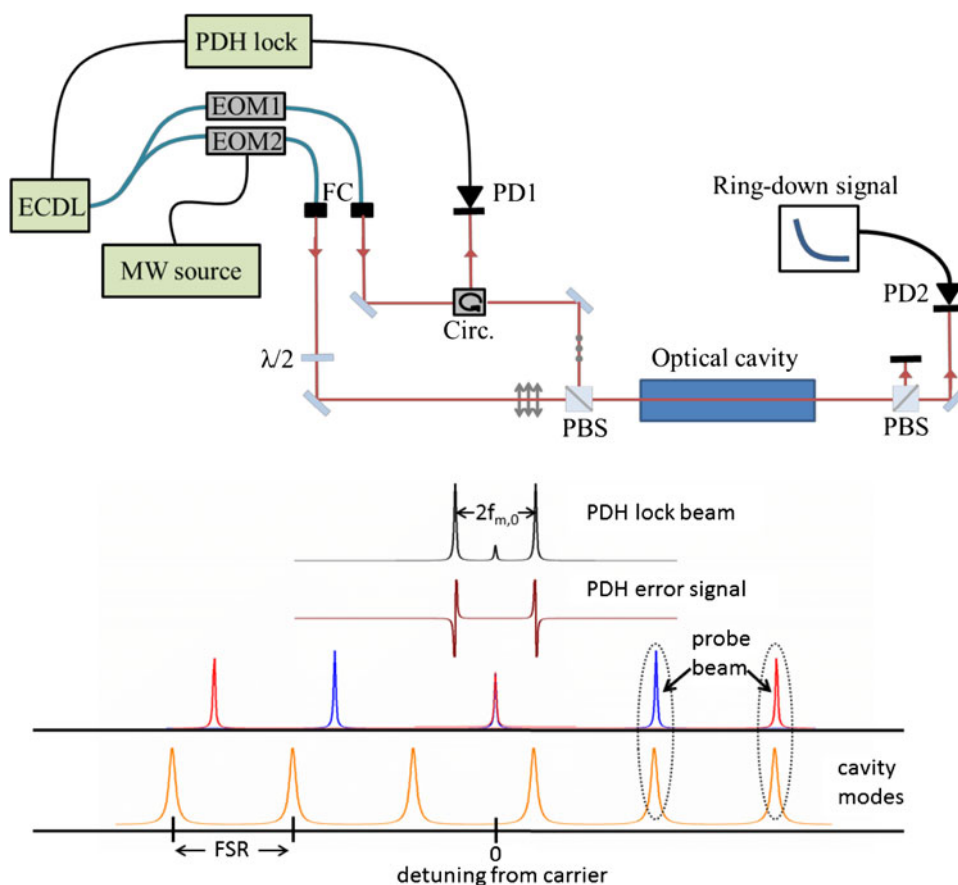
Fig. 1 Schematic and operating principles of the PDH-locked, dual-polarization FARS-CRDS spectrometer. The fiber-coupled, ECDL output is split into probe and locking beams. The locking beam is phase modulated with a waveguide electro-optic modulator (EOM1) at $f_{m,0} = 13$ MHz and then PDH locked to the optical cavity. This PDH lock is performed at $2f_{m,0}$ in order to lock one of the two sidebands to the cavity (so that the carrier frequency is nonresonant). Note that while the two beams are free space, they have orthogonal, linear polarizations. The probe beam is phase modulated with EOM2

at a microwave (MW) frequency such that a single, selected sideband is resonant with the optical cavity. This frequency can then be rapidly stepped by the MW source in increments of the cavity's free spectral range (FSR) in order to scan a molecular resonance. The probe leg laser spectrum is shown for two different values of f_{MW} in *blue* and *red*. Ring-down events are initiated by switching off the MW frequency of EOM2. The remaining shown components are photodiodes (PD), a circulator (Circ.), polarizing beam splitters (PBS) and free-space fiber couplers (FC)

Care was taken to minimize leak through of the lock beam on to the probe beam (i.e., ring-down) detector. The lock leg was aligned slightly off-axis into the cavity in order to facilitate spatial filtering. However, a small but detectable amount of light from the lock leg was still visible on the probe detector due to the finite extinction of the polarizing beam splitters. The use of higher extinction ratio polarization optics (e.g., Glan–Taylor polarizers) should reduce this effect and possibly improve our long-term averaging.

3 Results and discussion

For quantifying the sensitivity of the FARS-CRDS spectrometer, we measured the noise-equivalent absorption coefficient defined as

$$\text{NEA} = \frac{\sigma_\tau}{c\tau^2\sqrt{f_a}}, \tag{2}$$

where σ_τ is the standard deviation of the empty-cavity time constant $\tau \approx 16$ μs, c is the speed of light, and $f_a \approx 8$ kHz is the acquisition rate of the decay signals. We obtained a relative standard deviation in the time constants of $\sigma_\tau/\tau \approx 0.008$ % yielding an NEA of $\approx 1.7 \times 10^{-12}$ cm^{-1} Hz$^{-1/2}$ (see lower panel of Fig. 2 for an Allan deviation [18] plot for this system). Note that the relative standard deviation of our ring-down signals is more than an order of magnitude smaller than those generally achieved with high-sensitivity cw-CRDS (e.g., [13]). This measured value of σ_τ/τ is within a factor of ten of the shot-noise limited value, as given by

$$(\sigma_\tau/\tau)_{sn} = \sqrt{e/(P_0\tau\Re)}, \tag{3}$$

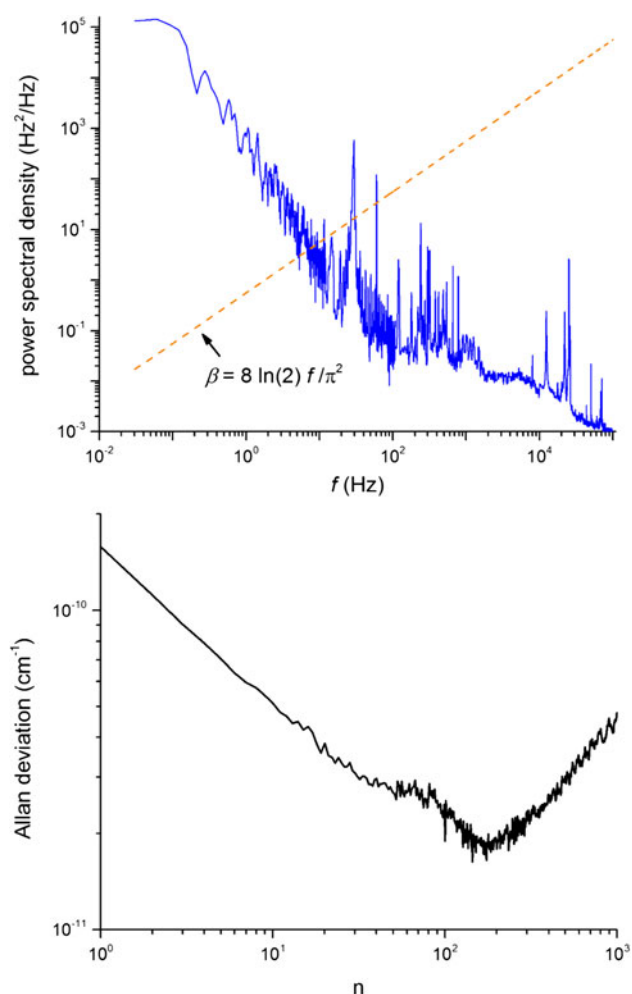**Fig. 2** (*Upper panel*) Power spectral density measurement used to calculate the relative linewidth of the PDH-locked ECDL. This linewidth is ~ 130 Hz full width at half-maximum (FWHM) and was approximated by integrating all regions where the PSD is greater than the function, $\beta = 8\ln(2)f/\pi^2$ known as the β-separation line [22]. (*Lower panel*) Allan deviation versus averaging number n, as a measure of the system's short-term stability. The minimum detectable absorption coefficient for a single ring-down measurement is 1.6×10^{-10} cm^{-1} which is reduced to 1.7×10^{-11} cm^{-1} after averaging 170 ring-down time constants (requiring 20 ms at an acquisition rate of 8 kHz)

Fig. 3 Series of ring-up and ring-down events recorded in real-time at a given laser frequency. The acquisition rate was ≈ 7 kHz and was limited by the cavity response time itself. The relative standard deviation of the measured ring-down time constants was ≈ 0.008 %

pumping the cavity and observing decay events. This high acquisition rate is enabled by the PDH locking of the ECDL to the ring-down cavity, which both narrows the laser's relative linewidth and leads to efficient optical pumping.

To the best of our knowledge, the NEA obtained in this experiment is the third lowest reported in the literature (see Table 1). Of these three cases, the lowest NEA was achieved using noise-immune cavity-enhanced optical heterodyne molecular spectroscopy (NICE-OHMS) [6]. The other was a CRDS measurement which used high-dynamic-range analog electronics to measure τ [5]. Most importantly, these two systems [5, 6] utilized cw-Nd:YAG lasers which offer high power, ultranarrow linewidths, and long-term frequency stability. However, these lasers have a tuning range of only ≈ 0.1 nm.

We also note that when NICE-OHMS has been performed with any other laser source, the performance of the technique has been significantly reduced, with the three best sensitivities approximately 3–4 orders of magnitude worse than those reported when using a cw-Nd:YAG laser [1, 4, 7] (see Table 1). The NEA reported here is thus the lowest which has been reported when using a widely tunable laser. Furthermore, we see no major technical barriers to the use of a higher finesse cavity (e.g., 100,000–200,000) which would likely provide a corresponding increase in sensitivity. We are presently developing this instrument.

As can be seen in Table 1, the sensitivity achieved herein with FARS-CRDS using an ECDL is an order of magnitude better than we previously achieved when

where e is the electron charge, P_0 is the peak power of the ring-down signal (≈ 100 μW), and $\Re$ is the photodetector responsivity (≈ 1 A/W). The finite extinction ratio of AOMs (-50 dB) has been shown to limit the precision with which τ can be determined in cw-CRDS [16]. As a result, we attribute our low σ_τ/τ and thus the improved NEA to the superior extinction offered by EOMs (nominally -80 dB).

As can be seen in Fig. 3, our ring-down signal acquisition rate is limited only by the cavity's intrinsic response time. Specifically, a complete ring-up/ring-down cycle has a period of $f_a^{-1} \sim 8\tau$ in which equal times are spent
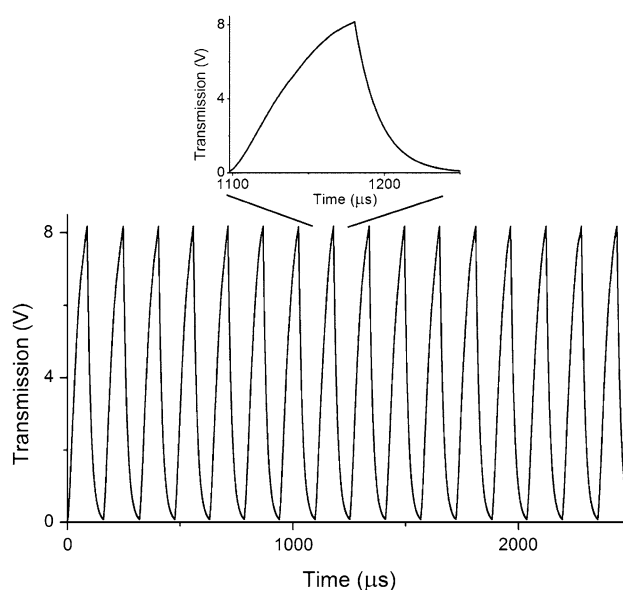
Table 1 Ultrasensitive cavity-enhanced techniques

Technique	Ref.	NEA (cm^{-1} $Hz^{-1/2}$)	Laser source	Tuning range (nm)
NICE-OHMS	[6]	1×10^{-14}	cw-Nd:YAG	0.1
CRDS	[5]	1×10^{-12}	cw-Nd:YAG	0.14
FARS-CRDS	Present	1.7×10^{-12}	ECDL	60
NICE-OHMS	[7]	5.6×10^{-12}	Fiber laser	1.0
CRDS	[4]	1.43×10^{-11}	Ti:sapphire	200
FARS-CRDS	[12]	2×10^{-11}	Fiber laser	1.0
NICE-OHMS	[1]	6.9×10^{-11}	ECDL	14
NICE-OHMS	[2]	8.5×10^{-11}	ECDL	50

The short-term, noise-equivalent absorption coefficient (NEA) and tuning range for the most sensitive cavity-enhanced spectrometers reported in the literature. These instruments are based upon either CRDS or NICE-OHMS. The frequency-agile, rapid scanning (FARS-CRDS) instrument reported herein offers the lowest NEA ever reported for a spectrometer with a tuning range >0.2 nm. We note that, unlike the case of FARS-CRDS, the NEA values given in the literature correspond to an operation at fixed wavelength and are significantly larger when these spectrometers are operated in scanning mode. The substantially higher scanning rate of FARS-CRDS is one of its largest advantages

utilizing an ultranarrow linewidth fiber laser. These two instruments both allowed for very high scanning rates (≈ 8 kHz) which were limited only by the cavity response time itself. However, the standard deviation of the measured ring-down time constants (σ_τ) was an order of magnitude lower when the ECDL laser was utilized, thus leading to the higher sensitivity. We attribute this higher sensitivity to the tighter lock we were able to achieve with the ECDL when utilizing the dual-polarization approach. While the fiber laser offers an ultranarrow linewidth, its frequency is controlled by a piezoelectric transducer which only allows for a few kHz of bandwidth due to strong mechanical resonances, thus limiting the maximum lock bandwidth and cavity transmission.

In addition to ultrahigh sensitivity, FARS-CRDS also permits high-bandwidth scanning. Because of the frequency agility of our microwave source, we are able to achieve a scanning rate of 8 kHz. As can be seen in Fig. 4, we are able to scan over a molecular resonance with, essentially, no measurement dead time. The shown spectrum was recorded in ≈ 2 ms.

Using the FARS-CRDS method, we have routinely achieved signal-to-noise ratios of several thousand to one for weak near-infrared absorption features (e.g., Figure 5). Furthermore, by recording the heterodyne beat signal between our optical carrier frequency and a self-referenced OFC, we are able to measure absolute transition frequencies. These measurements are directly linked to a cesium atomic clock to which our OFC is referenced. Near-infrared CO_2 transition frequencies can be recorded with standard uncertainties of ≈ 100 kHz from a single spectrum recorded in a few milliseconds. These uncertainties, which are dominated by uncertainty in fitting the line position and in measuring the heterodyne beat frequency, are more than an order of magnitude lower than those found in the HITRAN 2008 database [19]. Given the small relative line
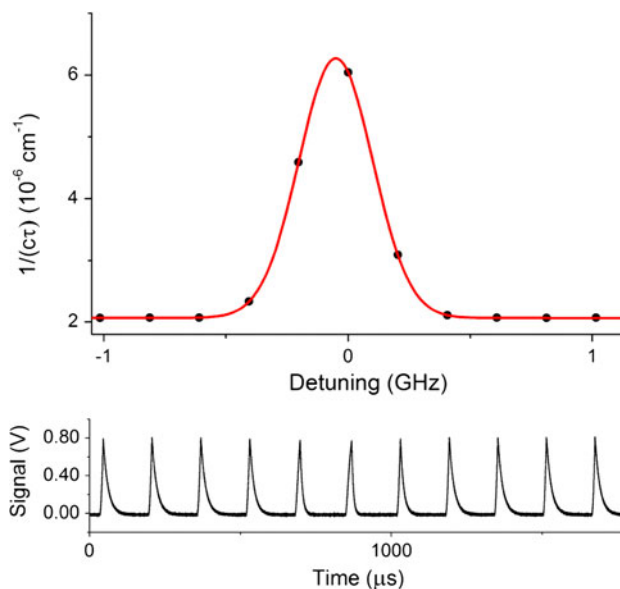

Fig. 4 (*Upper panel*) Measured absorption spectrum and speed-dependent Nelkin–Ghatak [23] fit of the (30012) ← (00001) P14e CO_2 transition centered at 6,336.242 cm^{-1} [20] for a pure CO_2 sample at a pressure of 12 Pa. (*Lower panel*) The corresponding real-time data acquisition. These 11 ring-down decays were acquired in ≈ 2 ms, corresponding to an acquisition rate of ≈ 6 kHz. During each ring-down decay, the microwave frequency was stepped by the cavity's free spectral range. As a result, each decay occurred at the corresponding frequency found in the *upper panel*. Note that due to the high absorption at *line center*, the corresponding ring-down decay occurs at a faster rate

width discussed above, the accuracy of the OFC frequencies and the long-term stability of the ring-down cavity lock (≈ 10 kHz), we expect averaging to yield kHz-level uncertainties in line position determinations. This level of performance was recently demonstrated in our laboratory using the comb-linked frequency-stabilized CRDS technique [20].
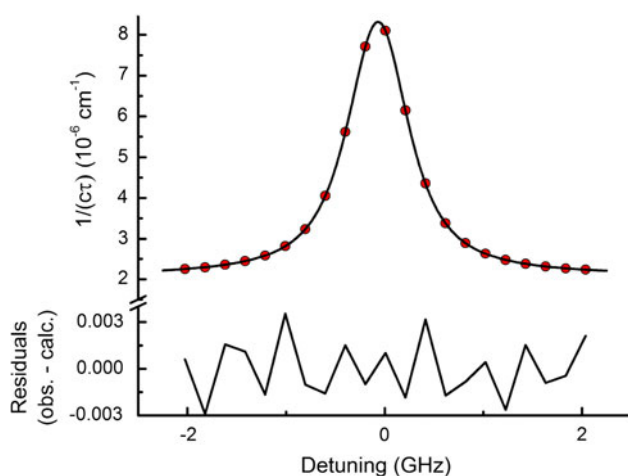
Fig. 5 Typical measured spectrum and speed-dependent Nelkin–Ghatak [23] fit of the $(30012) \leftarrow (00001)$ P14e CO_2 transition for a sample of CO_2 in air ($\approx 4{,}400$ μmol/mol) at a pressure of 13.3 kPa. The shown spectrum has a signal-to-noise ratio of 3,200:1 and is an average of 6 individual spectra each recorded in ≈ 2.6 ms

We note that the low relative linewidth (≈ 130 Hz) of our probe laser and the high accuracy of our microwave source allow us to record transmission spectra of individual cavity resonances (see the upper panel of Fig. 6). These mode-resolved cavity transmission measurements enable us to locate the center frequencies of the ≈ 10 kHz-wide resonances to within ≈ 1 Hz. This capability provides a low uncertainty determination of the cavity's free spectral range which is useful for generating the list of microwave scanning frequencies. In addition, linking these measurements to an optical frequency comb provides the measurements of intra-cavity and mirror dispersion.

Due to the equivalence of the time-domain and frequency-domain response of the ring-down cavity, an absorption spectrum could be derived from the FWHM of the Lorentzian cavity resonances which are given by $(2\pi\tau)^{-1}$ (see the lower panel of Fig. 6). This mode-resolved method differs from cavity-enhanced transmission techniques that measure the wavelength dependence of the peak transmission as opposed to the shape and width of the individual resonances (e.g., [21]). This mode-resolved transmission method offers a straightforward way to extend the dynamic range of a ring-down spectrometer, especially when large absorption losses preclude accurate time-domain measurements of decay rates.

4 Conclusions

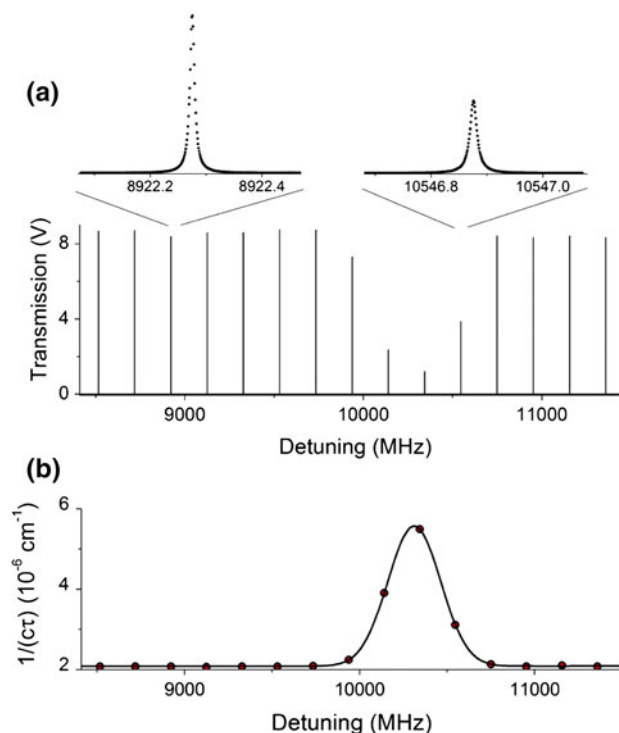We have presented a FARS-CRDS instrument which utilizes a commercially available, widely tunable ECDL. The

Fig. 6 a Transmission measurement of the cavity resonances. The ≈ 130 Hz relative linewidth of the probe laser (see the *upper panel* of Fig. 2) allows for the measurement of the individual cavity resonances (see *insets*). This technique allows for low uncertainty measurements of the cavity's free spectral range, which are used to set the frequencies of the microwave source. In addition, when linked to an absolute frequency reference, this technique allows for simultaneous measurements of the absorption (mode width) and dispersion (mode position) within the resonator. Finally, the widths of the cavity resonances yield an independent and consistent determination of the intra-cavity absorption spectrum. **b** Absorption spectrum of the P14e transition derived by measuring the width of the individual cavity resonances shown above. The relative uncertainty of the fitted width of the cavity resonances in the absence of molecular absorption was ≈ 0.04 %. The line intensities derived from this measurement agreed to those obtained from traditional cavity ring-down measurements to within 0.08 %

combination of a high-bandwidth locking approach and high optical extinction leads to a noise-equivalent absorption coefficient of 1.7×10^{-12} cm^{-1} Hz$^{-1/2}$. In addition, we have achieved scanning rates as high as 8 kHz. A minimum detectable absorption coefficient of 1.7×10^{-11} cm^{-1} was achieved in only 20 ms. We believe that FARS-CRDS offers an unprecedented combination of sensitivity, scanning rate and spectrum fidelity. Due to its generality and relatively low complexity, FARS-CRDS can be readily applied to many problems in trace gas sensing.

References

1. L. Gianfrani, R.W. Fox, L. Hollberg, J. Opt. Soc. Am. B **16**(12), 2247 (1999)
2. C. Ishibashi, H. Sasada, Jpn. J. Appl. Phys. **38** (2A), 920 (1999)
3. D.A. Long, A. Cygan, R.D. van Zee, M. Okumura, C.E. Miller, D. Lisak, J.T. Hodges, Chem. Phys. Lett. **536**, 1 (2012)
4. R.Z. Martinez, M. Metsala, O. Vaittinen, T. Lantta, L. Halonen, J. Opt. Soc. Am. B **23**(4), 727 (2006)
5. T.G. Spence, C.C. Harb, B.A. Paldus, R.N. Zare, B. Willke, R.L. Byer, Rev. Sci. Instrum. **71**(2), 347 (2000)
6. J. Ye, L.S. Ma, J.L. Hall, J. Opt. Soc. Am. B **15**(1), 6 (1998)
7. P. Ehlers, I. Silander, J. Wang, O. Axner, **29**(6), 1305 (2012)
8. V.M. Baev, T. Latz, P.E. Toschek, Appl. Phys. B **69**(3), 171 (1999)
9. Y. He, B.J. Orr, Appl. Phys. B **79**(8), 941 (2004)
10. H.F. Huang, K.K. Lehmann, J. Phys. Chem. A **115**(34), 9411 (2011)
11. I. Debecker, A.K. Mohamed, D. Romanini, Opt. Express **13**(8), 2906 (2005)
12. G.-W. Truong, K. O. Douglass, S. E. Maxwell, R. D. Van Zee, D. F. Plusquellic, J. T. Hodges, D. A. Long, Nature Photon. **7**, 532 (2013)
13. J.T. Hodges, H.P. Layer, W.W. Miller, G.E. Scace, Rev. Sci. Instrum. **75**(4), 849 (2004)
14. K. O. Douglass, S. E. Maxwell, G.-W. Truong, R. D. Van Zee, J. T. Hodges, D. A. Long, D. F. Plusquellic, In preparation (2013)
15. R.W.P. Drever, J.L. Hall, F.V. Kowalski, J. Hough, G.M. Ford, A.J. Munley, H. Ward, Appl. Phys. B **31**(2), 97 (1983)
16. H. Huang, K. Lehmann, Appl. Phys. B **94**(2), 355 (2009)
17. A. Cygan, D. Lisak, P. Maslowski, K. Bielska, S. Wojtewicz, J. Domyslawska, R.S. Trawinski, R. Ciurylo, H. Abe, J.T. Hodges, Rev. Sci. Instrum. **82**(6), 063107 (2011)
18. D.W. Allan, Proc. IEEE **54**(2), 221 (1966)
19. L.S. Rothman, I.E. Gordon, A. Barbe, D.C. Benner, P.F. Bernath, M. Birk, V. Boudon, L.R. Brown, A. Campargue, J.P. Champion, K. Chance, L.H. Coudert, V. Dana, V.M. Devi, S. Fally, J.M. Flaud, R.R. Gamache, A. Goldman, D. Jacquemart, I. Kleiner, N. Lacome, W.J. Lafferty, J.Y. Mandin, S.T. Massie, S.N. Mikhailenko, C.E. Miller, N. Moazzen-Ahmadi, O.V. Naumenko, A.V. Nikitin, J. Orphal, V.I. Perevalov, A. Perrin, A. Predoi-Cross, C.P. Rinsland, M. Rotger, M. Simecková, M.A.H. Smith, K. Sung, S.A. Tashkun, J. Tennyson, R.A. Toth, A.C. Vandaele, J. Vander Auwera, J. Quant. Spectrosc. Radiat. Transfer **110**(9–10), 533 (2009)
20. G.-W. Truong, D.A. Long, A. Cygan, D. Lisak, R.D. Van Zee, J.T. Hodges, J. Chem. Phys. **138**, 094201 (2013)
21. K. Nakagawa, T. Katsuda, A.S. Shelkovnikov, M. Delabachelerie, M. Ohtsu, Opt. Commun. **107**(5–6), 369 (1994)
22. N. Bucalovic, V. Dolgovskiy, C. Schori, P. Thomann, G. Di Domenico, S. Schilt, Appl. Optics **51**(20), 4582 (2012)
23. S.G. Rautian, I.I. Sobelman, Sov. Phys. Usp. **9**(5), 701 (1967)